Chapter 3
Unravelling Ribosome Function Through Structural Studies

Abid Javed and Elena V. Orlova

Abstract Ribosomes are biological nanomachine that synthesise all proteins within a cell. It took decades to reveal the architecture of this essential cellular component. To understand the structure-function relationship of this nanomachine needed the utilisation of different biochemical, biophysical and structural techniques. Structural studies combined with mutagenesis of the different ribosomal complexes comprising various RNAs and proteins enabled us to understand how this machine works inside a cell. Nowadays quite a number of ribosomal structures were published that confirmed biochemical studies on particular steps of protein synthesis by the ribosome. Four major steps were identified: initiation, elongation, termination and recycling. These steps lead us to the important question how the ribosome function can be regulated. Advances in technology for cryo electron microscopy: sample preparations, image recording, developments in algorithms for image analysis and processing significantly helped in revelation of structural details of the ribosome. We now have a library of ribosome structures from prokaryotes to eukaryotes that enable us to understand the complex mechanics of this nanomachine. As this structural library continues to grow, we gradually improve our understanding of this process and how it can be regulated and how the specific ribosomes can be stalled or activated, or completely disabled. This article provides a comprehensive overview of ribosomal structures that represent structural snapshots of the ribosome at its different functional states. Better understanding rises more particular questions that have to be addressed by determination structures of more complexes.

Synopsis: Structural biology of the ribosome.

Keywords Ribosome · Function · Structure · X-ray · cryoEM · Nascent chain

A. Javed · E. V. Orlova (✉)
Institute of Structural and Molecular Biology, Department of Biological Sciences, Birkbeck College, Malet Street, London WC1E 7HX, UK
e-mail: e.orlova@mail.cryst.bbk.ac.uk

A. Javed
e-mail: a.javed@mail.cryst.bbk.ac.uk

J. R. Harris and J. Marles-Wright (eds.), *Macromolecular Protein Complexes II: Structure and Function*, Subcellular Biochemistry 93,
https://doi.org/10.1007/978-3-030-28151-9_3

Why We Need to Study Ribosomes

Across all kingdoms of life, biological systems need proteins for their function. These proteins are encoded in their genomes. Specific nanomachines carry out translation of the genetic information into amino acid sequences of proteins. These bio-machines are named as ribosomes. Ribosomes decode the genetic information contained in a messenger RNA (mRNA) transcript and synthesise nascent polypeptide chains (NC), that will fold to become functional proteins.

In prokaryotes, ribosomes are dispersed in the cytoplasm, while in eukaryotes they can be both in the cytoplasm and can be bound to membranes of the nucleus and endoplasmic reticulum. Eukaryotes also have mitochondrial ribosomes, which translate mitochondrial proteins encoded in mitochondrial DNA. Depending on the cell type molecular mass of ribosomes varies from 2.5 to 4.5 MDa. Their sizes are characterised by Svedberg coefficients (S), which is a measure of a particle size based on its sedimentation rate in differential centrifugation. Prokaryotic ribosomes were named as 70S ribosomes, due to their lower S coefficient than eukaryotic ribosomes, which have the sedimentation coefficient of 80S (Taylor et al. 1967). In all organisms, ribosome consists of two ribonucleoproteins subunits (Tissieres and Watson 1958) (Fig. 3.1). The prokaryotic subunits are smaller and named as 30S and 50S whereas the eukaryotic ribosome subunits are termed as 40S and 60S respectively. Each subunit comprises of ribosomal RNA (16S for small and 23S for large subunits in bacteria) and 18S for small and 28S for large subunits (in eukaryotes) and ribosomal proteins (54 in bacteria and 80 in eukaryotes—Melnikov et al. 2012 and references herein) (Figs. 3.1 and 3.2).

The small subunit (SSU) of the ribosome binds the mRNA that contains the coded information of a protein to synthesise it. This step is followed by the formation of the ribosome/mRNA complex. The mRNA moves on the ribosome between the small and large subunit (LSU) where it is decoded (translated) with the assistance of different ribosomal factors into a sequence of amino acids. The SSU carries out one of the main ribosomal function such as decoding the mRNA and monitoring translation reliability. LSU operates a peptidyl transferase centre (PTC), where the polymerisation of amino acid into a new polypeptide chain takes place. Then the chain leaves the ribosome through the protein-exit tunnel. The data acquired by different studies revealed that the main steps of protein translation and formation of a polypeptide chain are profoundly conserved.

Due to the complexity of eukaryotic ribosomes and challenges in their purification from eukaryotic sources, bacterial ribosomes proved to be a good model

Fig. 3.1 Ribosome architecture. **a**—Bacterial ribosome (shown in grey) is composed of two subunits. The small subunit (SSU) is shown in gold, the large subunit (LSU) is shown in blue. Characteristic domains are labelled. **b**—the inter-subunit bridge points in SSU and LSU are shown (Liu and Frederick, 2016). **c**—components of ribosomal subunits located on the inner surface. **d**—components of the ribosome located on the outer surface of the ribosome. rRNA is shown in yellow (in SSU) or blue and dark blue (in LSU), and ribosomal proteins are shown in orange (SSU) or magenta (LSU) ▶

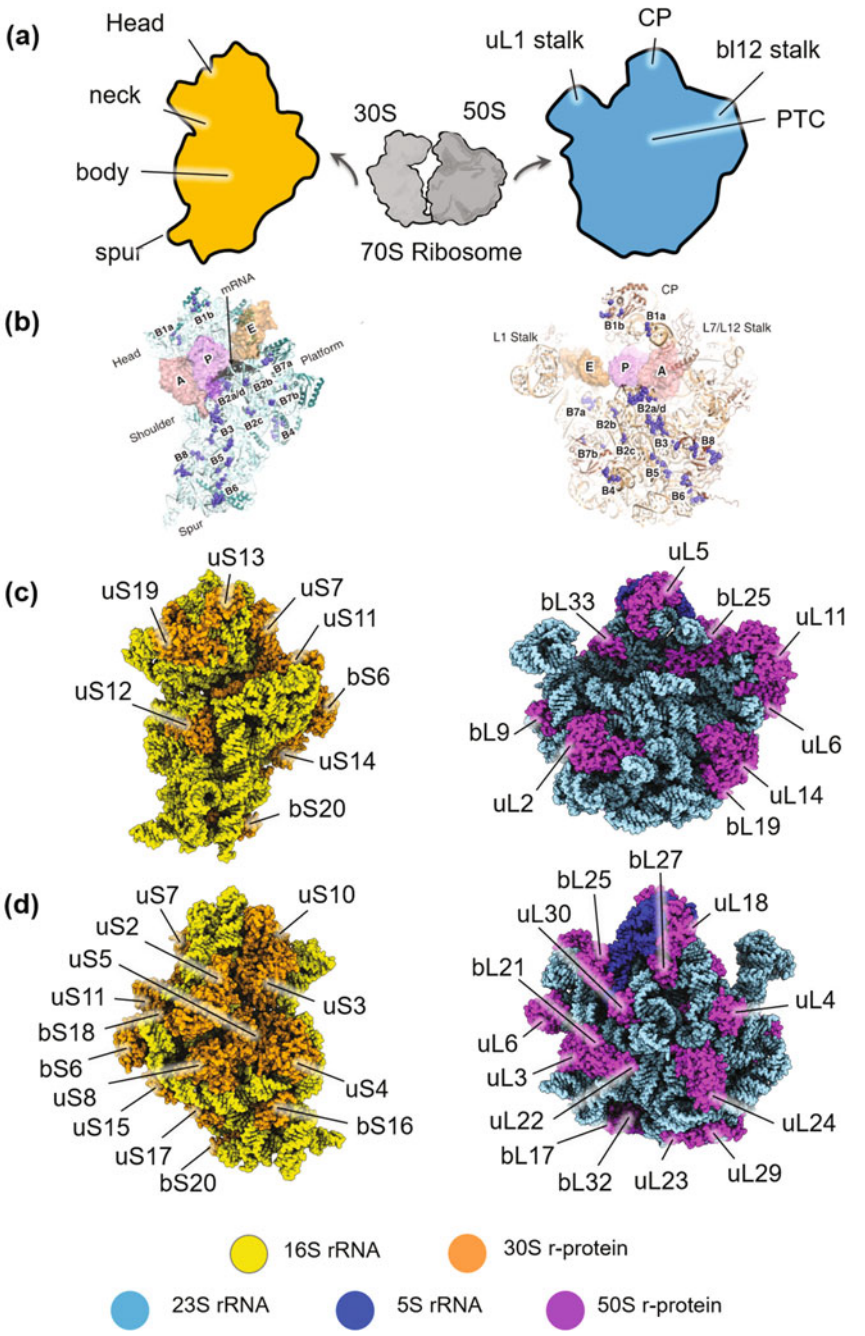
(a)
Head
neck
body
spur
30S
50S
70S Ribosome
uL1 stalk
CP
bl12 stalk
PTC
(b)
mRNA
Head
Platform
Shoulder
Spur
L1 Stalk
L7/L12 Stalk
(c)
uS13
uS19
uS7
uS11
bS6
uS12
uS14
bS20
uL5
bL33
bL25
uL11
bL9
uL6
uL2
uL14
bL19
(d)
uS7
uS10
uS2
uS5
uS11
uS3
bS18
bS6
uS4
uS8
uS15
bS16
uS17
bS20
bL27
bL25
uL30
uL18
bL21
uL4
uL6
uL3
uL22
uL24
bL17
bL32
uL23
uL29
16S rRNA
30S r-protein
23S rRNA
5S rRNA
50S r-protein

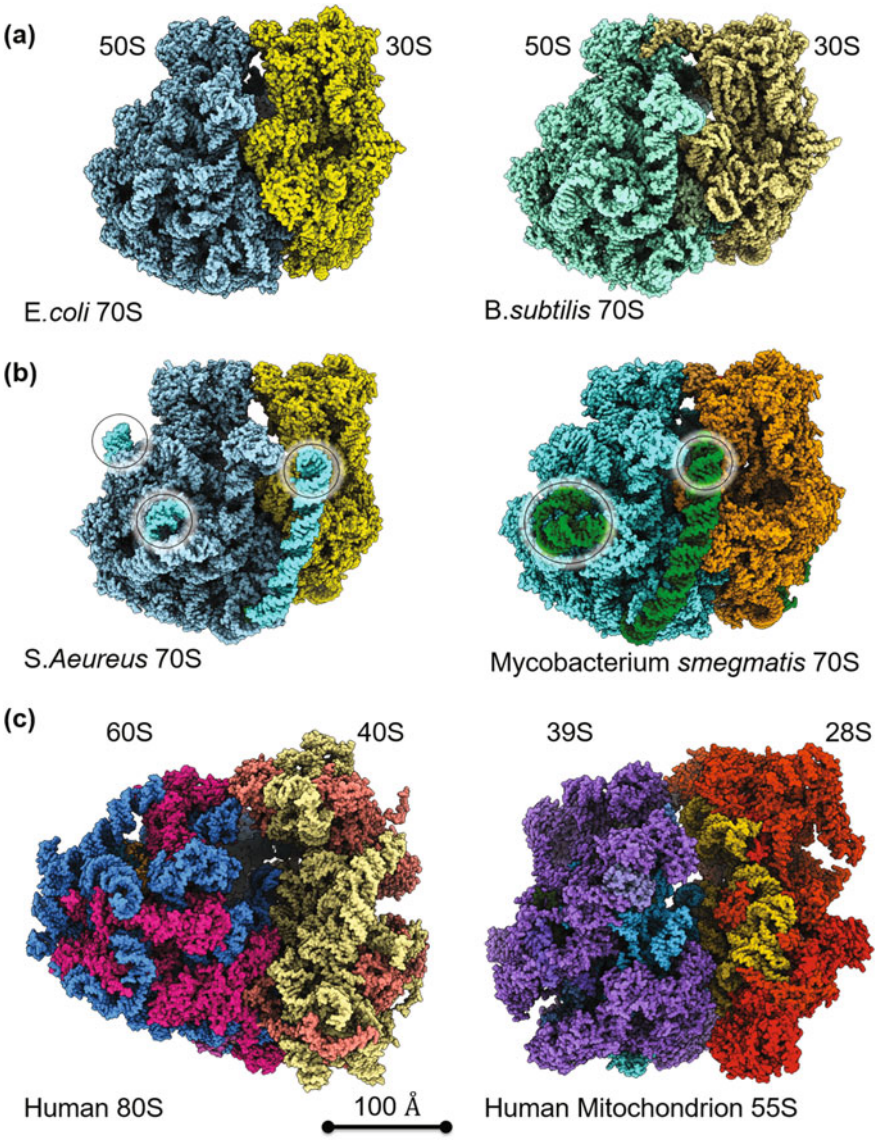

Fig. 3.2 Comparison of ribosomes from different organisms. **a**—*E. coli* 70S ribosome (PDB 4YBB) is shown with LSU in blue and SSU in yellow. The *B.subtilis* 70S ribosome (PDB 3J9M), very similar in structure to *E. coli* ribosome is shown with its LSU in cyan and SSU in pale yellow. **b**—The more divergent prokaryotic ribosomes are shown; ribosome structure from *S.aureus* (PDB 5NGM) and ribosome from *M.smegmatis* (PDB 5O61) shows rRNA extensions (circled and highlighted in blue or green). **c**—Eukaryotic ribosomes from human (PDB 4UG0) and mitochondrial 55S ribosome (PDB 3J9M). Human LSU rRNA is in dark blue and proteins in magenta whilst SSU rRNA is shown in pale yellow and proteins in orange. Mitochondrial LSU (39S) subunit rRNA is in blue and proteins in purple whilst SSU (28S) rRNA is shown in yellow and proteins in red. Scale bar is 100 Å

system to study ribosome structure and function and have contributed to a wealth of our existing knowledge of this complex nanomachine. Moreover, an extremely large number of diseases in mammals are caused by pathogenic bacteria. The leading tactic has been finding means to suppress these pathogenic microorganisms. Currently, usage of ribosome-specific antibiotics that will block translation in pathogenic ribosomes is the most efficient approach. The differences between prokaryotic and eukaryotic ribosome permits to use the antibiotics to block the activity of the bacterial ribosomes but allows mammalian ribosomes to function as normal. Furthermore, bacteria evolve much faster compared to the development of new specific drugs, leading to prevalent antibiotic resistance. Therefore, improvement in understanding structure-function relationship within ribosomes, particularly pathogenic prokaryotic ribosomes, became essential both in the sense of revealing crucial factors in the activity of these nanomachines and understanding specific mechanisms by which ribosome's activities are regulated.

Methods Used in Studies of Ribosome Structure/Function Relationship

The large size and complexity of the ribosome represented significant challenges for understanding their structural organisation, therefore a number of structural techniques were utilised to study the function of ribosomes. Ribosomes were discovered in the middle of the 1950s. Images of Palade particles were obtained by electron microscopy of stained thin sections of the rat pancreas where an unusual pattern of grains on the outer surface of the endoplasmic reticulum was reported (Palade 1955). Later these 'grains' were identified and renamed as ribosomes. Morphology and dimensions of these particles and individual subunits were assessed using negative stain EM (NS EM). The fully assembled ribosome particles have sizes ~250 Å for the 70S and ~250–300 Å for the 80S (Lake 1978; Bernabeu and Lake 1982). Then, the substantial impact for understanding their function came via extensive biochemical approaches that yielded illuminating insights into the essence of the ribosome function. Comparative DNA sequence analysis, sedimentation and SAXS methods have shown that the ribosome is a complex of ribosomal RNA (rRNA) with the well-ordered organisation and a number of globular proteins (r-proteins; Moore et al. 1968; Delius et al 1968; Noller and Herr 1974; Herr and Noller 1975; Brosius et al. 1978).

NS EM images of bacterial ribosomes revealed the basic structural features of the ribosome. These include the early description of ribosomal subunits. The SSU has four major structural domains: the "head" domain containing the major domain of rRNA, the "platform" with the RNA central domain, the "shoulder", and "foot" containing rRNA domain. Shoulder, foot and platform together form the "body" which is connected by the "neck" with the SSU head domain (Fig. 3.1a, left panel). The LSU of the prokaryotic ribosomes has been described as having a crown shape

characterised by three protuberances: “ridge”, “central” formed by 5S RNA and more elongated “stalks” on each side of the LSU: uL1, and bL12 stalks (Fig. 3.1a, right panel) (Frank and Agrawal 1998; Stark et al. 1997; Matadeen et al. 1999). Sample preparation by negative staining (NS) imaging, however, resulted in flattened molecular complexes (Orlova 2000; Frank 2006—and references herein), preventing to get reliable structural information on the ribosome, and the NS does not allow to see the details of the inner structure of the complex.

Studies on the individual components of the ribosome provided details of the overall organisation of this nano-machine. Neutron scattering studies of the individual subunits of bacterial ribosomes determined the relative positions of the ribosomal proteins (r-proteins) (Moore and Engelman 1975). Antibodies raised against the r-proteins located on the outer surface together with imaging using NS EM (immuno-electron microscopy) further localised some ribosomal proteins on both subunits on the surface (Tischendorf et al. 1974a, b). These observations were confirmed by chemical cross-linking studies on *E. coli* ribosome subunits, which provided details of r-protein-rRNA contacts (Moller and Brimacombe 1975).

Development of methods of bacterial ribosome purification commenced the quest for determination of a detailed architecture of this macromolecular machine by many research groups. X-ray crystallography has been known by that time as a routine technique for structural analysis of proteins at atomic resolution. Yet, ribosome represented an immense challenge for usage of this technique. A crucial prerequisite to have this method successful is the necessity of high-quality crystals and the size of the unit cell in these crystals. It took significant efforts and time until the first ribosome crystals were obtained for X-ray crystallography (Yonath et al. 1987). And, the process of obtaining a structure of the ribosome at an atomic resolution was not a well-paved road. It took nearly one third of the century to obtain atomic structures of ribosomes, with the help of other approaches.

Cryo-EM (cryo-electron microscopy at liquid nitrogen temperatures) is a fast-developing powerful tool used zealously in structural studies of macromolecular assemblies with molecular masses ranging from hundred KDa to MDa. Computational and technological advances extend boundaries of achievements by cryo-EM in structural studies of large bio-complexes and provide a wealth of information on the atomic level, assisting our understanding of functional mechanics and dynamics (Henderson 2015). Rapid freezing of thin layers of samples in liquid nitrogen enabled researchers to capture ribosomes in a near-native environment (Dubochet et al. 1988; Frank et al. 1991; Orlova 2000). The first structure of the bacterial 70S ribosome at nearly native conditions was obtained by cryo-EM in 1991 by Frank and colleagues. Electron crystallography of crystals of the chick embryo ribosome, and later low-resolution X-ray studies of *Bacillus stearothermophilus* 50S subunit indicated that there is a putative opening within the LSU for the exit of newly synthesised nascent polypeptide chains (NC) (Bernabeu and Lake 1982; Milligan and Unwin 1986; Yonath et al. 1987). The position of IgG antibody bound to the β–galactosidase NC in the NS EM images of the 80S translating ribosomes suggested that there is a channel through which the NC emerges from the ribosome (Bernabeu and Lake 1982). Further studies confirmed

the existence of the exit channel for the newly synthesized polypeptide chain (Frank et al. 1995; Beckmann et al. 1997; Ban et al. 2000; Gabashvili et al. 2000, 2001). The next step in functional studies of the ribosomes was provided by the revelation of structural conformations in ribosomes using computational methods in the analysis of cryo-EM images. This helped to analyse the intrinsic dynamics of the ribosome complexes (Gabashvili et al. 2000; Elad et al. 2008). Due to the versatility of cryo-EM, it became the major tool for structural analysis of ribosome complexes allowing to understand their structural dynamics.

Combined studies of the ribosome by X-ray crystallography and cryo-EM represented an amazing example where this complementation provided one of the most significant breakthroughs in understanding the function of the ribosome bio-machine. The first 9 Å structure of the LSU ribosome (H50S) was obtained for the ribosome of *Haloarcula marismortui*, where the X-ray data were phased using the intermediate resolution EM map of the ribosome (Frank et al. 1995; Ban et al. 1998). Later, the refined structure at 2.4 Å of the LSU provided atomic details of 23S and 5S ribosomal RNA, revealed locations of ribosomal proteins and suggested the structural basis behind the catalytic peptide bond synthesis at the PTC (Ban et al. 2000). The structure of the SSU from the eubacteria *Thermus thermophilus* subsequently demonstrated the loci of the mRNA and tRNA binding sites, previously indicated by low-resolution cryo-EM maps, that allowed to propose a mechanism of mRNA decoding (Gabashvili et al. 2000; Wimberly et al. 2000). At the same time, studies of the complete *Thermus thermophilus* 70S ribosomes at high-resolution of 5.5 Å provided insights on the mRNA-tRNA binding interface between subunits, elucidating a key role for the inter-subunit RNA bridges in keeping the LSU and SSU together during protein translation (Yusupov et al. 2001).

NMR spectroscopy is another method used to study the dynamic regions of the ribosome, enabling us to both undertake structural studies of complexes with a relatively small mass (less than ~40 KDa; Clore and Gronenborn 1998), and to study protein folding and dynamics of large biocomplexes. Using site-specific isotope labelling, this method helped to study the mobility of ribosome components such as ribosome stalk component bL12 (Fig. 3.1a, left panel) (Christodoulou et al. 2004) and ribosome-bound nascent polypeptide chains (Cabrita et al. 2016).

Novel approaches to decipher the ribosome structure and its dynamics are emerging and are used to expand our understanding of this complex molecular machinery (Fig. 3.1). Single-molecule fluorescence (smFRET) studies of the ribosome have provided details on movements of the ribosome elements during protein translation (Petrov et al. 2012) or spontaneous ribosome ratcheting as a result of higher temperatures (Cornish et al. 2008). Ribosome profiling is another powerful tool, proving successful to discern which proteins are translated when inside a cell (Ingolia et al., 2019). Combination of these methods is enabling us to reach deeper knowledge of the intricacies of ribosome structure and function.

General Organisation of Ribosomes in Prokaryotes

Genetic studies demonstrated that bacterial and eukaryotic ribosomes share a common structural core having two subunits SSU and LSU (Figs. 3.1 and 3.2). The SSU consists of 16S rRNA with 1458 nucleotides and 15 conserved proteins. The LSU has 19 conserved proteins, 5S rRNA and 23S rRNA, and ~4400 RNA bases related to the decoding site, PTC and tRNA-binding sites, which represent the major functional regions of the ribosomes. 16S and 23S rRNA form part of the mRNA channel on the small subunit and the exit channel on the large subunit, respectively (Schmeing and Ramakrishnan 2009; Melnikov et al. 2012). However, there are important differences in structural details, sizes and regulation of protein translation between ribosomes from prokaryotes and eukaryotes, and they vary between species. The differences between the ribosomes are defined by the presence of specific elements such as domain-specific proteins, insertions and extensions within the conserved proteins, and expansion segments of rRNAs that are defined by species and environment in which they exist (Melnikov et al. 2018). The 70S ribosome contains 20 bacteria-specific proteins (6 in the 30S subunit, 14 in the 50S subunit) and ribosomal RNA (Fig. 3.1). Most of these rRNA and proteins cover the main core from the solvent side and are accessible for interactions with translation factors and chaperones. The surface of the inter-subunit interface is composed predominantly of rRNA and, in the assembled ribosome, all functional sites are located close to this interface (Fig. 3.1).

Insights into the organisation of ribosomes from both Gram-negative and Gram-positive species have shown that the core of ribosome structure is highly conserved (Melnikov et al. 2018; Khusainov et al. 2016; Schmeing and Ramakrishnan 2009; Sohmen et al. 2015). At the same time, comparison of the pathogenic bacterial ribosomes demonstrated that there are varieties of the equivalent r-proteins, which apparently have evolved distinct functions due to specific adaptability of ribosomes (Fig. 3.2). For instance, r-protein bS1 on the SSU, which in *E. coli* is essential for translation initiation of canonical mRNAs comprises six RNA binding domains in *E. coli*; but its equivalent in *Sappylococcus. aureus* (*S. aureus*) (Fig. 3.2b, left panel) and other Gram-positive bacteria with low-GC nucleotide content have only four domains (Eyal et al. 2015; Khusainov et al. 2016). Moreover, there are indications that bacterial ribosomes may change their components according to the environmental alterations (Vesper et al. 2011). Across bacterial ribosomes, both 16S and 23S rRNA contain insertions (varying from *E. coli* ribosomes), which typically protrude from the ribosome to different extents (Fig. 3.2). For example, rRNA helices h6, h10, h26 and h44 in the SSU, and H28 and H68 in the LSU have different lengths or adopt different folds and orientations, as revealed when comparing the structures of 70S ribosomes from *E. coli and B. subtilis* (Fig. 3.2a, Noeske et al. 2015; Sohmen et al. 2015) and the structure of the 50S from *Staphylococcus aureus* (Eyal et al. 2015). Such variations in peripheral extensions suggest involvement in translation regulation at one or several stages of the process. Recently, a structure of the 70S ribosome of *Mycobacterium smegmatis*

(Fig. 3.2b, right panel), which is a close relative to the human pathogen Mycobacterium tuberculosis was solved by cryo-EM at 3.3 Å resolution (Hentschel et al. 2017). The structure has revealed two Mycobacterium specific ribosomal proteins in the vicinity of two drug-target sites in the catalytic centre (on the LSU) and the decoding site (on the SSU) (Hentschel et al. 2017). The bS22 protein is located on the 30S subunit between 16S and rRNA helices h27, h44, and h45 beneath the mRNA channel. The bL37 protein is sandwiched on the 50S between 23S and rRNA domain II (helices H39 and H40) and domain V (helices H72 and H89), which contains the universally conserved PTC and harbors the essential tRNA binding loops (A and P loops) (Ban et al. 2000; Hentschel et al. 2017). The structure of a pathogenic bacterial ribosome enabled differences to be discerned in the antibiotic binding sites on the ribosome that will eventually aid in designing mycobacterium specific antibiotics.

tRNAs are the non-ribosomal substrates that decode the genetic information and bring the amino acids that match to a codon in mRNA and should be incorporated in the growing protein. Ribosomal subunits have three binding sites for tRNA substrates: The A site where incoming aminoacyl-tRNA (A-tRNA) is bound, the P site holds the peptidyl tRNA (p-tRNA) corresponding to the codon and amino acid became attached to a nascent polypeptide chain during elongation, and the E site, at which the deacylated P-site tRNA, after peptide formation, became released from the (Schmeing and Ramakrishnan 2009). Analysis of the ribosome conformations through classification of EM structures helped to unveil key functional regions on the ribosome including the mRNA channel on the SSU, binding sites for A-, P- and E-tRNAs and their movement along the 70S ribosome during translation (Fig. 3.1b) (Frank et al. 1995; Agrawal et al. 1996, 2000). At each elongation cycle, both subunits participate dynamically in translocating the mRNA and the tRNA molecules by a single codon (Bashan and Yonath 2008). Consequently, cryo-EM has demonstrated one of the characteristic ribosome motions known as the "ratcheting" of the subunits, as such movement ensures shifts along the mRNA transcript during translation (Frank and Agrawal 2000).

Structural Basis of Protein Synthesis by the Ribosome

The main function of the ribosome is to decode mRNA and synthesise proteins. Four main steps were distinguished in the process of protein synthesis by the ribosome: initiation, elongation, termination and recycling. The SSU mediates base-pairing interactions between the mRNAs and tRNA that define the amino acid sequence of the nascent polypeptide chain while the LSU catalyses peptide bond formation at the peptidyl transferase centre (PTC) between the amino acids covalently attached to tRNA during elongation (Schmeing and Ramakrishnan 2009; Steitz 2008; Moore 2009). Structures of ribosome complexes captured at various stages of translation solved by cryo-EM and X-ray crystallography provided much of our understanding of how this translational machinery works.

Initiation

Translation initiation is an important cellular checkpoint that ensures the timely production of proteins. In bacteria, this step involves the consecutive formation of three intermediate complexes that differ both in composition and conformation. In essence, the SSU binds the mRNA close to the translation start site (Fig. 3.3). The initial fMet-tRNA binds to the first codon of the mRNA at the P-site and the next tRNA, which enters the ribosome at the dynamic bL12 stalk, attaches to the next codon at the A-site. As soon as a peptide bond is formed, the A-site tRNA is translocated to the P-site and the deacylated tRNA moves from the P-site to the E-site on its way out of the ribosome through the mobile uL1 stalk (Fig. 3.3). Several structures of translation initiation intermediates have been determined by X-ray crystallography and cryo-EM (Fig. 3.3—McCutecheon et al. 1999; Carter et al. 2000; Myasnikov et al. 2005; Marzi et al. 2007; Simonetti et al. 2008; Julian et al. 2011; Lopez-Alonso et al. 2017), providing key insights on how this important step that commences protein translation.

The first step is the formation of "30S pre-initiation complex" (30S PIC) that is composed of mRNA, fMet-tRNA and three initiation factors (Fig. 3.3a, b). X-ray structure of T. *thermophilus* 30S bound to mRNA mimic (containing Shine-Dalgarno (SD) sequence at the 5′ end of mRNA) provided details on how the SD sequence of mRNA docks at the 30S during initiation located between the 'head' and 'platform' domains of the SSU (Fig. 3.3b; Kaminishi et al. 2007). This interaction fixes the SD sequence of mRNA on SSU positioning the AUG start site at the P-tRNA binding site (Fig. 3.3c, d). Structural snapshots captured using single-particle cryo-EM, visualised mRNA structures in its folded and unfolded forms on the SSU and provided details on how SSU recruits the correct mRNA sequence during initiation (Marzi et al. 2007).

The 30S subunit has to bind mRNA and fMet tRNA at a correct 'match' that transforms the pre-initiation complex into the initiation complex (Fig. 3.3b). There are three non-ribosomal factors that participate in this process: initiation factor 1 (IF1), IF2, and IF3. IF3 and IF1 are involved in the mRNA adjustment process, ensuring the correct mRNA codon is selected before the ribosome enters the elongation phase (Fig. 3.3c). IF2 takes care of recruitment of fMet-tRNA to the ribosome in the "30S initiation complex" (30S-IC) (Fig. 3.3d), correct positioning of fMet-tRNA at the P-site in 70S-IC, and dissociation of IFs from 70S initiation complex (70S-IC) (Fig. 3.3e), using energy from GTP hydrolysis. A recent cryo-EM structure of an antibiotic (GE81112) stalled SSU pre-initiation complex with IF1, IF2 and IF3 and f-Met tRNA bound to 30S was reported (Lopez-Alonso et al. 2017). The study revealed conformational changes that occur on the SSU, binding of IF1, IF2, and IF3 on three distinct sites on the SSU and the changes in positions of fMet-tRNA, critical to start active 70S ribosome assembly and protein translation (Fig. 3.3d; Lopez-Alonso et al. 2017).

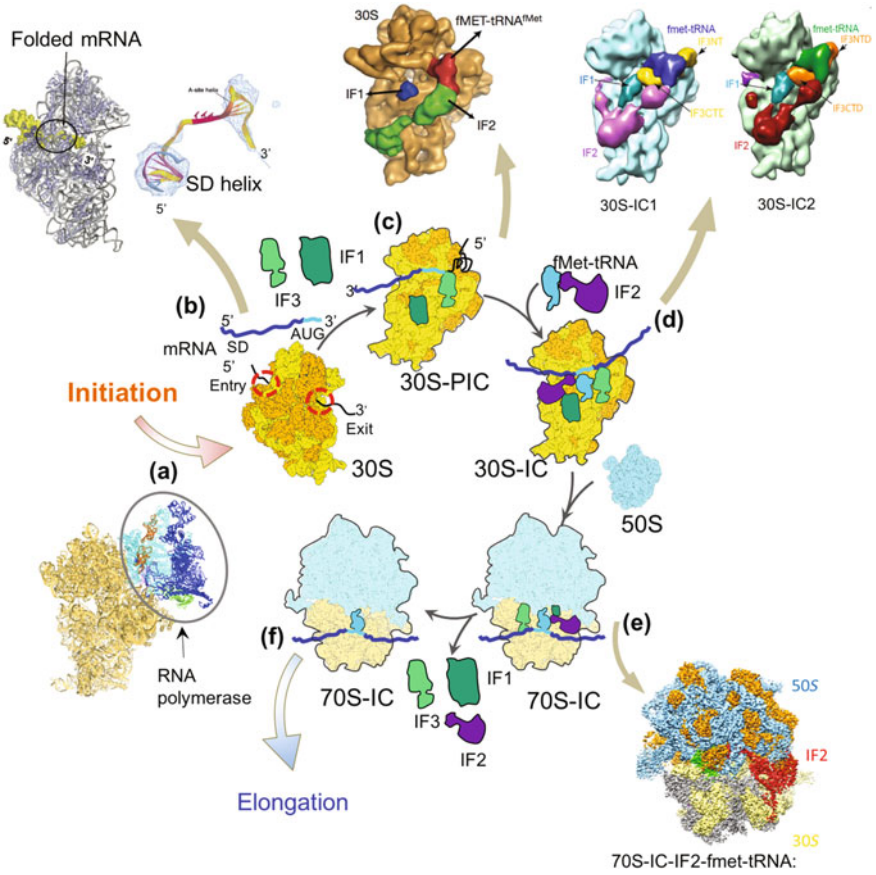

Fig. 3.3 Ribosome translation initiation. A schematic representation of bacterial translation initiation. **a**—The process begins with SSU (in yellow) coupled to mRNA synthesis by RNA polymerase (shown in blue) (Demo et al. 2017a, b). **b**—mRNA entry and exit on the SSU head are shown in red and the structure of mRNA with SSU shows the path mRNA takes on the SSU (Yusupov et al. 2001). Shine Dalgarno (SD) site on mRNA is indicated in the insert and AUG codon (start site) is shown in light blue on the mRNA. **c**—Initiation involves initiation factors: IF1 (in dark green), IF2 (purple) and IF3 (in light green) which bind the SSU to form pre-initiation complexes. **d**—The components that form these complexes are indicated: SSU in orange with fMet tRNA in red, and IF1 in blue and IF2 in green (Marzi et al. 2003); SSU in blue with IF1 in turquoise, IF2 in magenta and IF3 in yellow (Lopez-Alonso et al. 2017). **e**—Recently solved cryo-EM structure revealed how the last step of IF2 dissociation occurs (Sprink et al. 2016). **f**—Once LSU binds, the initiation factors dissociate to form the active 70S complex

Cryo-EM structure of 30S IC complex, comprising SSU, mRNA, fMet-tRNA and the three IF proteins shed light on how this conformational switch takes place, depending on the positioning of initiation substrates on the SSU (Julian et al. 2011). This was complemented by the structure of 30S-IC (lacking IF3), comprising 30S subunit, fMet-tRNA, IF1, IF2 and 27 nucleotide long mRNA. The structure

demonstrated the organisation of 30S-IC, showing how the tRNA is stabilised by IF2 and provides details on the interaction between the SSU and initiation factors (Simonetti et al. 2008). The results reveal that the 30S IC complex has IF2 bound close to mRNA channel and blocking A tRNA binding site on SSU; IF2 has contacts with IF1 (bound closer to P tRNA binding site), the 30S subunit shoulder, and the CCA end of fMet-tRNA, which occupies an intermediate (P/I) tRNA binding position (Fig. 3.3d). The N-terminal domain of IF3 contacts the tRNA, whereas the C-terminal domain is bound to the platform of the 30S subunit (Julian et al. 2011). Interactions of IFs with SSU ensure the accurate position of the tRNA anticodon to AUG start site on the mRNA at the SSU P-site (Simonetti et al. 2008; Julian et al. 2011).

Consequently, the LSU (50S) is attached to the 30S-IC leading to the formation of the 70S-IC, which is ready to enter elongation phase (Schmeing and Ramakrishnan 2009) (Fig. 3.3e, f). IF2 plays a key role in this structural transition from 30S-IC to 70S-IC, leading to dissociation of IF1 and IF3. The cryo-EM structure of 70S-IC-IF2-GDP (Fig. 3.3e) has disclosed how IF2 induces IF dissociation from 70S-IC upon GTP hydrolysis (Myasnikov et al. 2005). This structure demonstrates that in the GTP-analog bound state, IF2 interacts with SSU and initiator tRNA at the P-site inducing structural changes in IFs and the ribosome, leading then to the dissociation and release of IF dissociation and formation of active 70S-IC (Myasnikov et al. 2005). IF3, which regulates the correct mRNA and tRNA match was also found to remain bound to 70S-IC, even after subunit joining. The high dissociation rates measured biochemically measured implicated the factors involvement in alternative (non-SD led) pathways that possibly exist in translation initiation (Goyal et al. 2017).

The interaction between the SSU and LSU takes place via 12 bridges between the subunits, made by RNA–RNA, RNA–protein, and protein–protein interactions (Yusupov et al. 2001; Selmer et al. 2006; Korostelev et al. 2006; Harms et al. 2001; Shaikh et al. 2014; Noeske et al. 2015) (Fig. 3.1b). Bridge B2a is particularly important because it connects the elements of the LSU and SSU at the decoding centre of the SSU and the region that forms the PTC on LSU. The B2a bridge has the ability to adopt several conformations, depending on the functional state of the ribosome (Ban et al. 2000; Bashan et al. 2003). At the end of the initiation process, an active 70S-IC is formed which can start peptide bond formation (Fig. 3.3f).

Elongation

After initiation, ribosome begins protein synthesis in a process called elongation that consists of well-defined cyclical steps (Fig. 3.4). The elongation cycle includes decoding, movement of tRNA to the P-site to form peptide-bond, amino acid polymerisation, detachment of the P-site tRNA from the growing polypeptide chain and release of the deacylated tRNA (Fig. 3.4). These actions are governed by the successive coordinated movements of the mRNA, associated tRNAs between the

SSU and LSUs from A-site to the P-site and then to the E-site, one codon at a time (in a 3′ to 5′ direction), and interactions between amino acids forming a nascent polypeptide chain (NC). Upon peptide bond formation, the ribosome fluctuates between two major conformations: from a non-rotated to a rotated state (the SSU rotates counterclockwise with respect to the LSU on ~ 10° between two positions). The non-rotated state has the two tRNAs bound to P and A sites on both SSU and LSU whereas the rotated state has tRNAs bound in hybrid P/E and A/P conformers (LSU/SSU).

Decoding

The ribosome nanomachine operates with high precision to ensure correct matching of the tRNA anticodon with the mRNA codon on the A-site. This process is assisted by Elongation Factor-Tu (EF-Tu) that delivers aminoacyl-tRNAs to the ribosome. EF-Tu is bound to GTP and has a high affinity for aminoacyl-tRNA; together these three components form the ternary complex (Fig. 3.4a). Binding of the ternary complex to the A-site tRNA and the ribosome involves the flexible bL12 stalk on the ribosome, tethering a charged tRNA close to the ribosomal A site. This step is codon-independent (Kothe et al. 2004; Diaconu et al. 2005). Then the aminoacyl-tRNA bound to EF-Tu and A-site at the ribosome undergoes verification via correspondence of its anticodon with the mRNA codon. Once the correct match is found between the mRNA and A-site tRNA, EF-Tu hydrolyses GTP, reducing the affinity to aminoacyl-tRNA and enabling EF-Tu to dissociate from the ribosome (Fig. 3.4b). Cryo-EM studies of EF-Tu on the ribosome show that it contacts the shoulder domain of the SSU. The closure of the shoulder domain of the SSU moves it towards the ternary complex stabilizing the transition state for GTP hydrolysis by EF-Tu and leading to activation of the GTPase if the matching with codon was correct (Ogle et al. 2002; Ogle and Ramakrishnan 2005; Stark et al. 2002; Valle et al. 2003). X-ray structure of the 70S ribosome-EF-Tu-A-tRNA complex further highlighted distortions introduced in A-site tRNA that permit aminoacyl-tRNA to interact with both the decoding centre of the SSU and EF-Tu at the factor-binding site (Schmeing et al. 2009). This distortion is necessary for the tRNA to be accurately positioned at the PTC, close to the P-site tRNA (Fig. 3.4b) (Schmeing et al. 2009). Latest developments in cryo-EM image analysis methods enabled researchers to distinguish micro-heterogeneity in ribosome complexes captured during decoding. In particular, intermediate structures of 70S-EF-Tu-Asite tRNA complex were solved by cryo-EM revealing the link between codon recognition and the activation of translational GTPases steps on ribosomes (Loveland et al. 2017). Classification of large datasets (between 500,000 and 1 million particles) has shown a series of short living states reflecting the differences during the selection of cognate and near-cognate tRNA matches at the A-site. These structures demonstrated that at the correct codon match, the SSU undergoes a conformational change and binds tightly EF-Tu. Structures of near-cognate complex fail to induce conformational changes in the SSU required for anchoring of the aminoacyl-tRNA on the ribosome (Loveland et al. 2017).

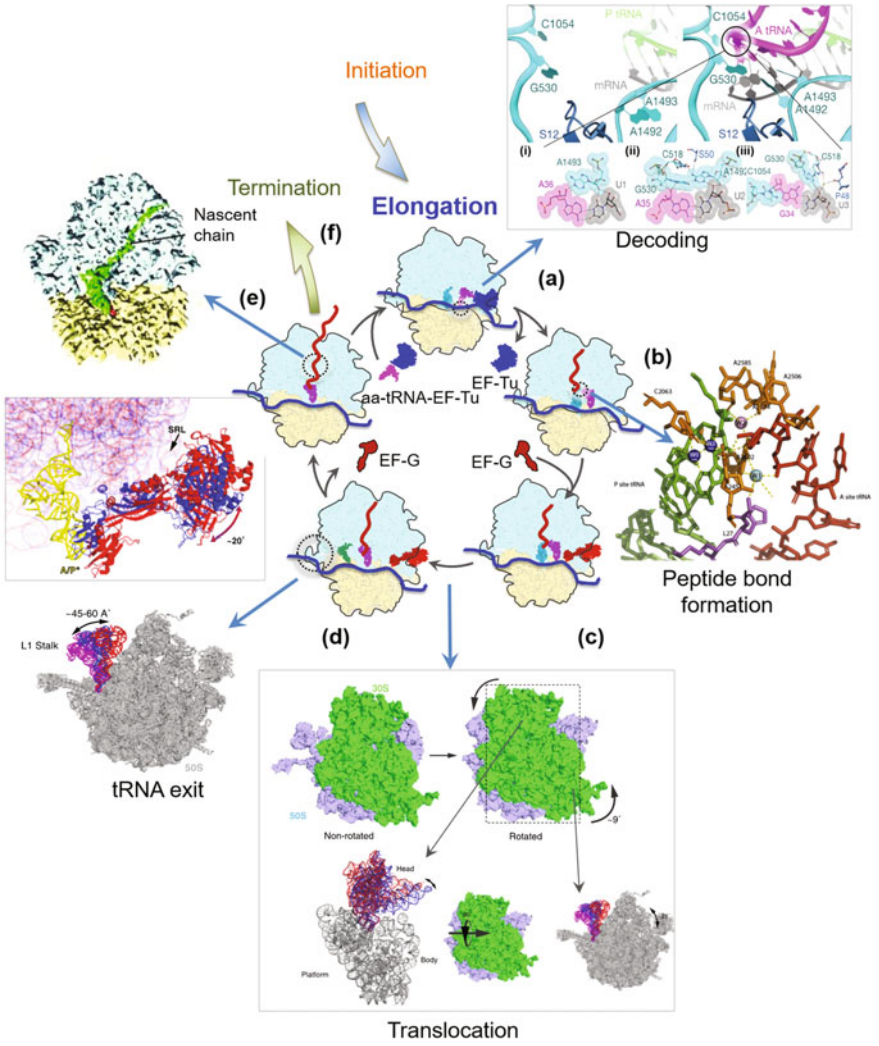

Fig. 3.4 Elongation cycle. The elongation starts as soon the 70S-fMet-tRNA complex is formed. **a**—The first step involves EF-Tu (in blue) bringing and binding the A-site amino-acid (magenta) for mRNA code recognition and selection—an insert shows structural details of the decoding and selection mechanism on the ribosome (adopted from Schmeing and Ramakrishnan 2009). **b**—Once the correct amino acid is selected, peptide bond formation occurs. The insert shows the P-site (green) and A-site tRNA (red) arrangement within the peptidyl transferase centre, surrounded by catalytic water molecules (W1-3) (Polikanov et al. 2014). **c**—EF-G (in red) then binds to catalyse the movement of tRNA and mRNA along the ribosome. **d**—The SSU physically moves ('ratcheting') with respect to the LSU. The insert shows non-rotated and rotated states of the 70S ribosome—the rotated SSU movement in head, shoulder and body domains (Ling and Ermolenko 2016). **e**—To allow E-site tRNA to exit, uL1 stalk (insert panel—Ling and Ermolenko 2016) moves inwards (highlighted as magenta to red). Upon GTP hydrolysis, EF-G dissociates (zoom in panel highlighting motions of EF-G in red and blue, after translocation and GTP hydrolysis), enabling the cycle to repeat and producing a nascent chain, emerging through the ribosome exit tunnel on the large subunit (zoom in panel—NC in green; Seidelt et al. 2009)

Peptide Bond Step

After the release of EF-Tu, the aminoacyl-tRNA moves form A-site to the active site of protein synthesis on the LSU known as the peptidyl transferase centre (PTC). The peptidyl tRNA (P-site tRNA) and aminoacyl-tRNA (A-site tRNA) react to form a peptide bond. The active site is located on nucleotides (domain V) from 23S rRNA. Several research groups during the early 90s undertook experiments to characterise the role of rRNA in the functioning of the PTC using biochemical and genetic screening. Mutational, footprinting, and crosslinking studies suggested the central loop of domain V 23S rRNA is involved in ribosome's peptidyl transferase activity (Polacek et al. 2001; Green and Noller 1997). These were subsequently verified by the high-resolution structures of the LSU.

Crystal structure of the archaea ribosome LSU confirmed that the PTC consists of nucleotides from domain V of 23S rRNA (Ban et al. 2000; Polacek and Mankin 2005). These structures of the ribosome indicated that the PTC active site is located at the bottom of a large cleft the LSU below the central protuberance (Ban et al. 2000; Harms et al. 2001; Noeske et al. 2015). The PTC cavity is formed by nucleotides of the central loop of domain V of 23S rRNA, and no ribosomal proteins were found in contact with the active site, confirming the suggestion that ribosomal enzyme activity is performed exclusively by rRNA. However, loops and long "tails" of ribosomal proteins uL2, uL3 and uL4 protrudes into the core of the ribosome (Nissen et al. 2000; Ban et al. 2000). It was proposed that ribosomal proteins located close to the PTC and tunnel entrance are essential for catalytic and regulatory rRNA activity. The structures also indicated that water molecules play an important role in interactions of the rRNA, tRNA and amino acid chemical groups within the active site during peptide bond formation (Polacek and Mankin 2005; Rodnina 2018).

During peptide synthesis at the PTC, carbonyl and amino groups from the amino acids attached on the ends of A- and P-site tRNA are positioned within the active site of the PTC at the LSU interface, where their universally conserved CCA ends are oriented and held in place by interactions with 23S rRNA (Fig. 3.4b; Yusupov et al. 2001). Peptide bond between the A-site amino acid and P-site amino acid is made when the α-amino group of the A-site aminoacyl-tRNA attacks the carbonyl group of P-site bound peptidyl tRNA (Fig. 3.4b). This chemical reaction at the PTC, producing the de-acylated tRNA at the P-site consisting of the de-acylated tRNA at the P-site and peptidyl-tRNA carrying an additional amino acid (+1 aa) at the A-site of the LSU (Fig. 3.4; Polacek and Mankin 2005).

mRNA and tRNA Translocation

Upon peptide bond formation and deacylation of P-site tRNA, ribosome participates in the translocation of tRNAs and mRNA between two subunits. This translocation requires the ribosome machinery to be adaptable enough to make the movement of tRNAs and mRNA smooth. Elongation factor G (EF-G) participates actively in this process providing energy for translocation. Several structures have revealed details on how mRNA, tRNA, and the ribosome interact to ensure re-adjustment of the components during translocation and preparing the whole complex for another round of elongation cycle (Schmeing and Ramakrishnan 2009;

Rodnina 2018). Translocation of the tRNAs and the mRNA on the ribosome is a multi-step process representing a great challenge to discern the intermediates states when tRNAs and mRNA move relative to the subunits of the ribosome. Current structural models complemented by results from an ensemble and single-molecule kinetic studies using a large variety of fluorescence reporters and fluorescence resonance energy transfer (FRET) pairs distinguished up to eight discrete steps (Guo and Noller 2012; Adio et al. 2015; Belardinelli et al. 2016; Wasserman et al. 2016). Contrary to the view that EF-G is essential for the movement of mRNA and tRNA, a recent crystal structure of ribosome in complex with mRNA and two tRNAs shows a spontaneous movement of mRNA and tRNAs from pre-translocation to post-translocation state, without the presence of EF-G (Zhou et al. 2019). This suggests that the movement of mRNA and tRNAs is facilitated by the ribosome itself.

During translocation, the SSU and LSU move relative to each other in the motion now known as 'ratcheting' where subunits rotate forward and reverse in a cyclical manner in a plane parallel to the inter-subunit interface. Furthermore, the 'head' domain of SSU carries out forward- and back-swivelling motions with respect to the body of the SSU around the axis is perpendicular to the inter-subunit plain (Fig. 3.4). These movements are essential to power movement of mRNA and tRNAs between the SSU and LSU. The ribosome ratchet motion was first visualised and described in the low-resolution cryo-EM structures of the ribosome translocation complex, providing the first evidence that interactions with the ribosome drive the substrate movements during elongation (Frank and Agrawal 2000). Subsequent high-resolution structures of the elongation pre-translocation and post-translocation complexes provided a visual picture of how elongation takes place (Rodnina 2018).

After EF-G binding to the ribosome, the SSU head and body domains move in the counter-clockwise direction relative to the large-subunit, which corresponds to the direction of translocation and accompanied by hydrolysis of GTP (Guo and Noller 2012; Belardinelli et al. 2016; Wasserman et al. 2016). Subsequently, the SSU body begins moving backwards in the clockwise direction, whereas the head remains in the forward-swivelled state (Guo and Noller 2012; Belardinelli et al. 2016; Wasserman et al. 2016) (Fig. 3.4c, d). This opens the decoding region allowing to uncouple the tRNAs from the interactions with the ribosome elements that hold the mRNA and the tRNA anticodons in the A and P site, respectively. Disconnection of the codon–anticodon complexes from the SSU moves 30S head domain to the non-rotated state (Guo and Noller 2012; Belardinelli et al. 2016; Wasserman et al. 2016). The tRNAs are then precisely positioned at the P and E sites and the EF-G is released (Fig. 3.4e; Savelsbergh et al. 2003).

Structures of post-translocation 70S ribosome demonstrate movements of the uL1 stalk, which acts as a sensor towards deacylated P-tRNA and moves by nearly 40 Å to help tRNA to exit from E-site and out from the ribosome (Schmeing and Ramakrishnan 2009; Rodnina 2018). Movements of both subunits, together with EF-G, display the mechanism of the ribosome that allows mRNA and tRNA to reposition and proceed to the next elongation cycle.

Termination

Once the ribosome reaches a stop codon on the mRNA, elongation (synthesis of the nascent chain) is completed. In bacteria, stop codons are recognized by the termination (or release) factors RF1 and RF2, which read the codons UAG/UAA and UGA/UAA, respectively (Fig. 3.5a). The third termination factor, RF3, regulates activities of RF1 and RF2 but is not required for peptidyl-tRNA hydrolysis. The process of termination consists of three main steps: recognition of the stop codon, hydrolysis of the ester bond of the peptidyl-tRNA (with the assistance of RF1 or RF2), and dissociation of RF1/RF2 with the help of RF3 (Fig. 3.5b). RF1 and RF2 select the respective stop codons by conserved recognition peptide motifs: "P-V-T" in RF1 or "S-P-F" in RF2 (Schmeing and Ramakrishnan 2009; Rodnina 2018).

Structures of ribosome termination complexes were determined by X-ray and cryo-EM that show that there are conformational changes in RF which trigger the termination of translation (Fig. 3.5; Schmeing and Ramakrishnan 2009). It was found that domain 1 of RF2 interacts with the uL11 stalk of the 70S ribosome (Korostelev et al. 2008; Weixlbaumer et al. 2008); however, this interaction is broken in complexes with RF1 bound (Fig. 3.5b, inserts) (Korostelev et al. 2008; Laurberg et al. 2008). This finding indicates that recognition of the stop codon is distinct for each RF. The sm-FRET studies also supported the fact that RF1 and RF2 stabilise the ribosome in the non-rotated state (Rawat et al. 2003, 2006; Korostelev et al. 2008, 2010; Laurberg et al. 2008; Weixlbaumer et al. 2008; Santos et al. 2013), whereas RF3 alone stabilizes the rotated state (Gao et al. 2007; Jin et al. 2011).

X-ray structure of a mutated RF1 bound to 70S suggested a mechanism of RF1 activation upon ribosome binding (Svidritskiy and Korostelev 2018). In the structure, RF1 catalytic domain was bound outside the PTC whilst the codon-recognition domain of RF1 was bound to the stop codon, accompanied with structural re-arrangements in the SSU decoding centre (Svidritskiy and Korostelev 2018). This suggests that RF1 recognises stop codon which induces conformational changes in SSU that cause the release of mRNA and tRNA.

In instances where ribosomes are stalled on a non-stop encoded mRNA (or truncated mRNA) caused by in-complete transcription or cellular stress, bacterial cells rescue these ribosomes by encoding ArfA factor (James et al. 2016; Huter et al. 2017a, b; Demo et al. 2017a, b). Cryo-EM studies of ribosomes in complex with ArfA, RF2, mRNA and tRNAs provided an insight on how ArfA, together with RF2, rescue stalled ribosomes. ArfA is able to identify ribosomes that have no mRNA in the 30S mRNA channel and recruits RF2 to mediate NC release from the ribosome, resulting in stalled ribosomes to terminate translation and to be recycled (Fig. 3.5a, left panel—Demo et al. 2017a, b).

Upon the release of NC, RF3 (with GTP hydrolysis) facilitates dissociation of remaining substrates: RF1 and RF2 from the ribosome, leaving tRNA in a hybrid P/E state and mRNA on the ribosome (Figs. 3.5b, c). Cryo-EM structures of 70S-RF1-RF3 complexes provided information on how RF3 activates release factor

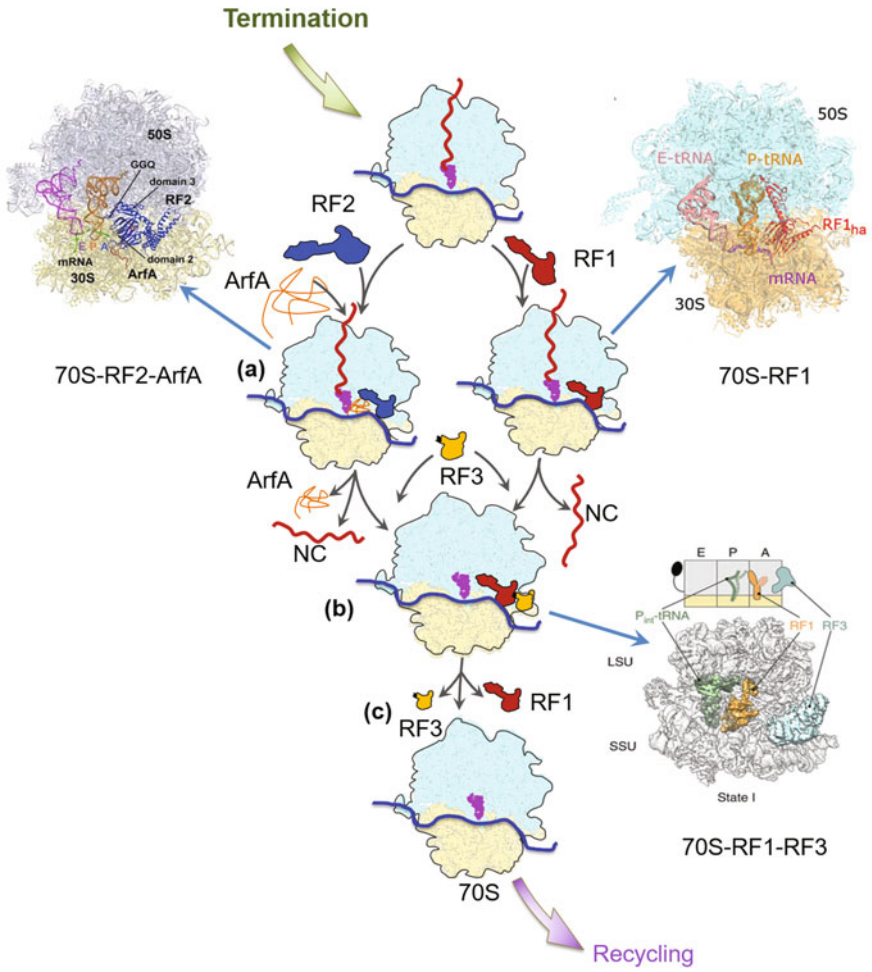

Fig. 3.5 Scheme of translation termination. Once a STOP codon is reached on the mRNA, the ribosome enters translation termination. **a**—Two factors: RF1 (in red) and RF2 (in blue) catalyse translation termination. For ribosomes that are stalled by non-stop codon mRNA (or truncated mRNA) for termination, an additional factor called ArfA (in orange) binds, together with RF2 to assist the ribosome termination. Left and right insert panels show recently solved cryo-EM strutures of 70S ribosomes with RF2 and ArfA (Demo et al. 2017a, b) and 70S with RF1 (Svidritskiy and Korostelev 2018). **b**—RF3 (in light orange) then binds the ribosome in either RF1 or RF2 bound states to catalyse the release of NC (red), as well as the RF1/RF2 bound to the ribosome. Cryo-EM structures of these complexes are shown in inserts: on the right is 70S bound with RF1-RF3 (Graf et al. 2018). **c**—Factors RF1 and RF3 dissociate from the ribosome, leaving hybrid P/E tRNA and mRNA on the ribosome followed by recycling

dissociation. The structures show that RF3 is recruited via bL12 stalk of the ribosome (Fig. 3.5c; Pallesen et al. 2013). Intermediate structures captured by cryo-EM show that binding of RF3 to the ribosome results in SSU head rotation and swivelling that shift the P-tRNA to hybrid P/E-site (Fig. 3.5c, right insert panel) (Graf et al. 2018). RF3 also induces rotation of the SSU that enables release of RF1 from its binding site. GTP hydrolysis of RF3 then enables RF3 to be released from the ribosome and for the subunits to be recycled (Fig. 3.5d) (Graf et al. 2018).

Recycling

In order for the ribosome to start a new round of protein synthesis, the post-termination 70S ribosome needs to be recycled: split into the individual subunits and be disassociated from mRNA and tRNA. In bacteria, the ribosome subunit separation is catalysed by the ribosome recycling factor (RRF) and EF-G. RRF binds to the A site of the ribosome (Gao et al. 2005) and stabilizes the SSU rotated with respect to the LSU in which the P-site tRNA in the hybrid P/E binding state (Dunkle et al. 2011). RRF consists of two domains (I and II), which interact with the LSU and SSU (Fig. 3.6; Fu et al. 2016).

Once EF-G and RRF dissociate the ribosome into subunits, binding of IF3 to the SSU prevents re-association of the SSU and LSUs (Peske et al. 2005; Zavialov et al. 2005). The mechanism by which both EF-G and RRF cooperate to induce ribosome recycling has remained less well-understood for a long time. Using time-resolved cryo-EM Fu et al. (2016) were able to obtain structural snapshots of short-lived intermediate states of ribosome recycling (Fig. 3.6a, b; Fu et al. 2016). The authors pre-incubated 70S post-termination ribosomes with RRF and then rapidly mixed them with EF-G, IF3, and GTP before spraying the sample onto a cryo-EM grid. Using classification of particle images several structures of ribosome recycling complexes were obtained at medium resolution, ranging between 7 and 20 Å. The 70S-EF-G-RRF complex provided information on how domain 4 of EF-G contacts domain 2 of RRF inducing separation of subunits (Fig. 3.6b). In the absence of EF-G, RRF moves closer to inter-subunit rRNA disrupting the bridge B2a (Fig. 3.6c). These experiments enabled authors to capture the post-termination complex of the LSU-EF-G-RRF complex, after dissociation from the SSU. The structure obtained shows RRF domain 1 in close proximity to H69 domain of 23S rRNA, in comparison to 70S-EF-G-RRF complex (Fu et al. 2016). Altogether, the structural snapshots illuminate a mechanism by which bacterial ribosomes undergo subunit splitting and recycling, ready until the next translation cycle begins.

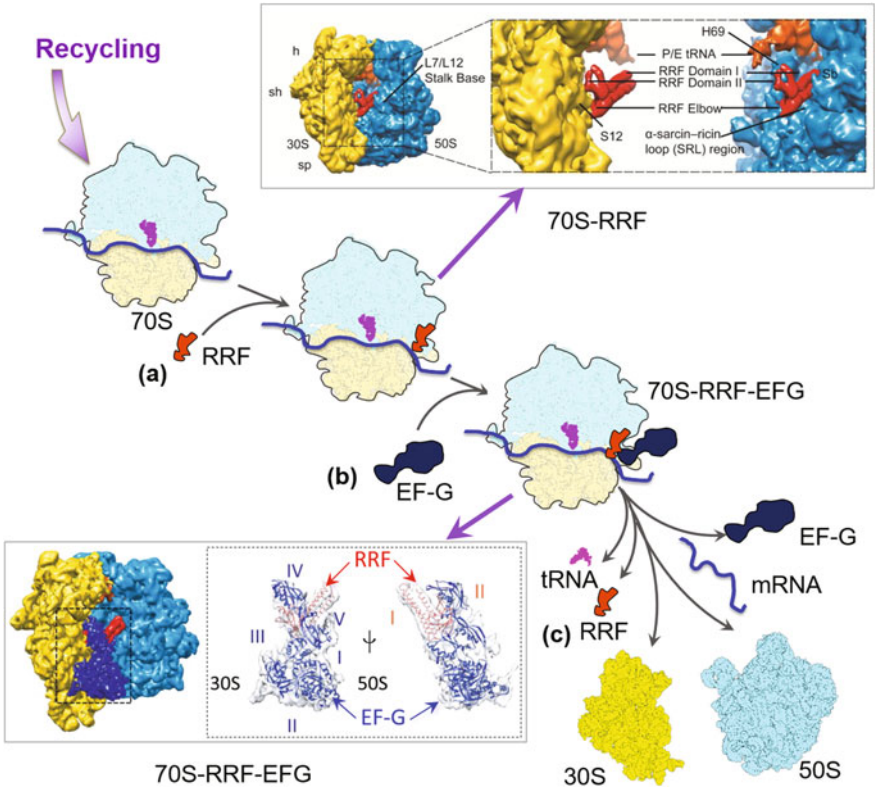

Fig. 3.6 Schematic diagram of ribosome recycling. **a**—Ribosome recycling factor (RRF—in red) recognise 70S ribosome with tRNA and mRNA followed by termination. **b**—Together with EF-G (blue) it catalyses the dissociation of the two subunits. **c**—Cryo-EM structures identifying structural intermediates during this process are shown in inserts: Top right panel shows structures of the 70S bound to RRF only (Fu et al. 2016) and the bottom panel shows the subunits dissociation in the last step of recycling, as the RRF, EFG, tRNA and mRNA leave the ribosome (Fu et al. 2016)

Regulatory Co-translational Events at the Ribosome Exit Tunnel

The ribosome has the ability to monitor the progress of translation and modulate nascent peptide chain (NC) folding by coupling with the speed of translation. During elongation, the NC moves through the exit tunnel of the ribosome. The exit tunnel is about 100 Å long with an average diameter of 15 Å that can accommodate a chain of ~30 amino acids before the NC emerges from the ribosome. The NC can start folding within the tunnel during elongation, accommodating secondary structure elements or even from small domains (Nilsson et al. 2015, 2017; Tian et al. 2018). Recent cryo-EM structures of the NC small domains on stalled

ribosomes showed that folding of immunoglobulin domains can begin at the vestibule and close to tunnel exit (Nilsson et al. 2017; Tian et al. 2018; Javed et al. 2019 and references herein). NMR results confirm the fact that large domains fold primarily close to or outside the ribosome tunnel, during translation (Cabrita et al. 2016). The rate of the NC folding depends on interactions between the peptide emerging from the exit tunnel and the surface of the ribosome (Deckert et al. 2016). There is a link between sequence, number of rare codons in the mRNA, the rate of translation and the NC folding. These factors affect translation, alters the kinetics of co-translational folding, and changes the distribution of protein conformations in the resulting mature protein pool (Clarke and Clark 2008; Tsai et al. 2008; Zhang et al. 2009; Siller et al. 2010; Spencer et al. 2012; Yu et al. 2015; Buhr et al. 2016). Computational experiments modelling a process of folding on the ribosome suggest that the translation rate affects local folding rates and may induce or prevent mis-folding (O'Brien et al. 2014). The ribosome also acts as a hub during elongation coordinating co-translational events such as the NC folding with the recruitment of chaperones, and NC-modifying enzymes (Javed et al. 2017 and references herein).

To analyse interactions between the ribosome and NC during translation, one has to have the ribosome in a fixed, "semi" translational, state. Such a state is named as a stalled state of the ribosome. Cells have devised ways to achieve this by having non-stop mRNA sequence (or truncated mRNA) or by encoding short peptide sequences that interact with the exit tunnel and stall ribosomes (Javed et al. 2017; Wilson et al. 2016). One of the structurally characterised stalling peptides is the 17 residue SecM from bacterial secretion monitor protein, which regulates the expression of SecA translocon protein. Cryo-EM structures of SecM stalled ribosomes show specific points of interaction between the nascent peptide and the tunnel elements (rRNA and proteins) that define the strength of stalling (Bhushan et al. 2011). Small molecule drugs and antibiotics can stall the ribosome. EM structures of such stalled complexes demonstrated that these small molecules bound to the ribosome at the beginning of the tunnel close to PTC are triggering conformational changes blocking the channel (Li et al. 2018; Arenz et al. 2016). The speed of translation can also be slowed down by short repeat sequences of proline residues, translation of which stall the ribosome (Doerfel et al. 2015). To relieve poly-proline stalled ribosomes, bacterial cells express a specialised elongation factor (EF-P; Doerfel et al. 2015). Recent cryo-EM structures of EF-P bound ribosomes show that EF-P enters the E site of the ribosome and acts by bringing the P- and A-site substrates closer towards their catalytically productive orientation in the peptidyl transferase centre (Huter et al. 2017a, b). Altogether, the exit tunnel plays an important role during protein translation in monitoring events related to ribosome function in order to perform smooth production of the nascent polypeptide chain.

Future Prospects

Elucidation of the function of the ribosomes has come a long way due to the complexity of the ribosome and multitude of the factors involved into its function. The major accomplishments were made by amalgamation of biochemical and structural methods: X-ray crystallography, cryo-EM and NMR spectroscopy (Fig. 3.7). During the last decade, structural studies of bio-complexes progressed tremendously due to advances in computational technology and software development. That enabled us to gain a massive bulk of information on small details and essential conformational changes within the ribosome itself and in its complexes with assistant factors. The library of ribosomal structures determined using cryo-EM and X-ray crystallography allowed us to derive functional/structural relationship of this biological nanomachine (Fig. 3.7). Advances in automation of data collection in cryo-EM and software in statistical analysis particle images helped researchers to distinguish multiple states of ribosomes and extend characterisation of these nanomachines from gram negative bacterial ribosomes such as *E. coli* to gram positive and pathogenic bacterial, followed by analysis of eukaryotic ribosomes (Eyal et al. 2015; Hentschel et al. 2017). Obtaining high-resolution structures of non-characterised pathogenic bacterial ribosomes will help us map regions within the ribosome where existing antibiotics can be assessed for efficacy as well as the design of new effective antibiotics that can effectively block protein translation more widely.

The progress in studies of prokaryotic ribosomes paved the road to more systematic and efficient studies of much larger ribosome complexes and eukaryotic ribosomes, previously elusive or hypothesised based on biochemical studies. New areas in the understanding of the protein synthesis machine include analysis of properties, activity, and folding of the translation product, nascent polypeptide chain. It was long known that bacteria couple mRNA synthesis (i.e. the activity of RNA polymerase) to protein synthesis (i.e. ribosome protein translation). Yet the details of how RNA polymerase interacts with ribosome remains to be fully understood. Therefore, complexes of the RNA polymerase and the ribosome represent a special point of interest; how the RNA polymerase cooperates with ribosomes to couple bacterial transcription-translation and where is the link that makes such complex efficient in bacteria. Recent cryo-EM structures shed some light on this partnership between RNA polymerase and the ribosome (Demo et al. 2017a, b; Kohler et al. 2018). Nevertheless, how this coupling functions inside the cell remains to be seen. Particularly when ribosomes translate proteins inside a cell in polysomes (multiple ribosomes on a single mRNA) rather than as single ribosomes, many aspects of ribosome activity will require analysis of ribosomes and ribosome complexes in a cellular context.

Latest cryo-EM structures highlight the role of the ribosome also during co-translational folding of polypeptide chains as they emerge from the exit tunnel. Further structural analysis of ribosome-nascent chain complexes within cells will illuminate aspects related to the tuning of co-translational protein folding to

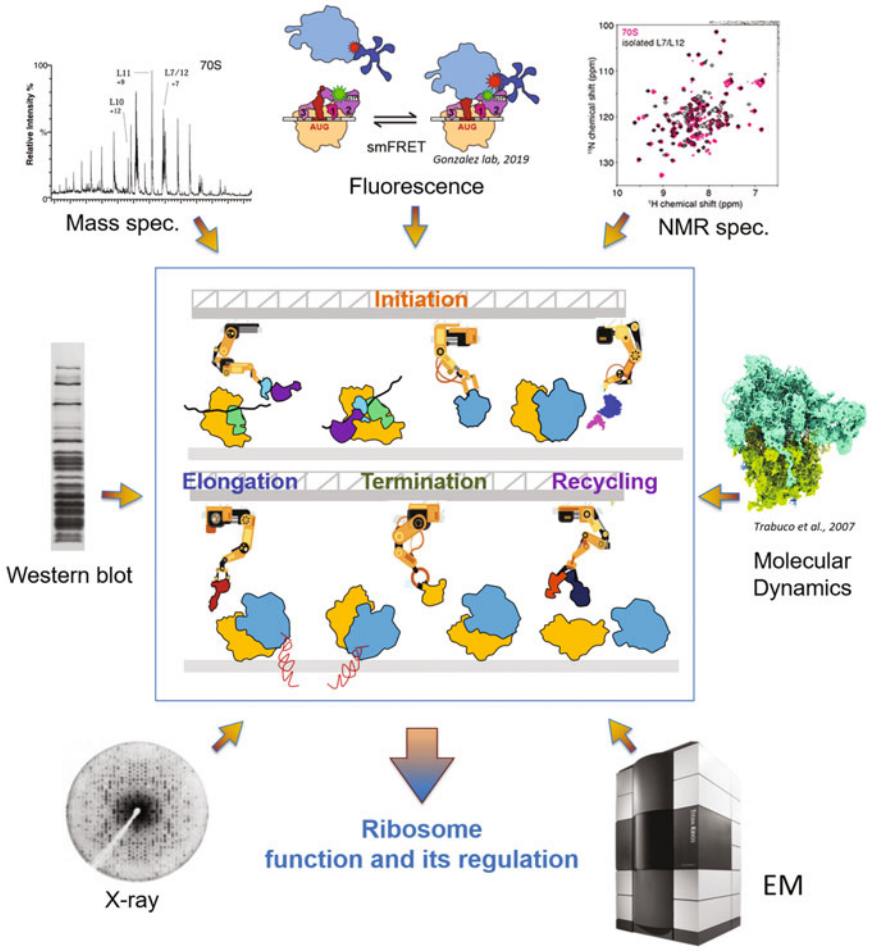

Fig. 3.7 Analysis of structure-function of the ribosome. Central panel (outlined in blue) shows the four major steps of translational (ribosomal subunits shown in yellow for 30S and blue for 50S, together with a variety of translation factors). Usage of different techniques (outlined as panels) illuminate the ribosome function as a nanomachine

activities of the ribosome. Both X-ray crystallography and cryo-EM can provide structures of intermediates of ribosomes, revealing many aspects of ribosome function. These intermediates however have to be artificially trapped, either by using antibiotics or peptides (Wilson et al. 2016). Undertaking structural studies in a time-resolved fashion without the use of antibiotics or non-hydrolysable GTP analogues will enable us to follow ribosome motions as they happen in real-time. A forthcoming method in this respect is time-resolved cryo-EM (Frank 2017), that is able to capture transient intermediates of ribosome complexes. For instance, analysis of molecular dynamics of ribosome machinery by time-resolved cryo-EM

captured intermediate states of elongating ribosome (Fischer et al. 2010; Chen et al. 2015), particularly short-lived intermediates that give rise to ribosome subunit dissociation during ribosome recycling (Fu et al. 2016). An improvement of the time resolution of single-molecule techniques may yield additional, yet uncharacterized transient intermediates, as recently demonstrated by (Fu et al. 2016). We envisage the combination of these methods mentioned above will come into force revealing many important intermediate states of the ribosome complexes during protein translation.

Acknowledgements A. J. is supported by BBSRC grant BB/R002622/1. We would like to thank Dr. D. Houldershaw for the computational assistance in structural analysis and software used.

Competing Financial Interests

The authors declare no competing financial interests.

References

Adio S, Senyushkina T, Peske F, Fischer N et al (2015) Fluctuations between multiple EF-G-induced chimeric tRNA states during translocation on the ribosome. Nat Commun 6:7442. https://doi.org/10.1038/ncomms8442

Agrawal RK, Spahn CM, Penczek P et al (2000) Visualization of tRNA movements on the *Escherichia coli* 70S ribosome during the elongation cycle. J Cell Biol 150(3):447–460

Agrawal RK, Penczek P, Grassucci RA et al (1996) Direct visualization of A-, P-, and E-site transfer RNAs in the *Escherichia coli* ribosome. Science 271(5251):1000–1002

Arenz S, Bock LV, Graf M et al (2016) A combined cryo-EM and molecular dynamics approach reveals the mechanism of ErmBL-mediated translation arrest. Nat Commun 7. https://doi.org/10.1038/ncomms12026

Ban N, Freeborn B, Nissen P et al (1998) A 9 A resolution X-ray crystallographic map of the large ribosomal subunit. Cell 93(7):1105–1115

Ban N, Nissen P, Hansen J et al (2000) The complete atomic structure of the large ribosomal subunit at 2.4 Å resolution. Science 289:905–920

Bashan A, Agmon I, Zarivach R et al (2003) Structural basis of the ribosomal machinery for peptide bond formation, translocation, and nascent chain progression. Mol Cell 1:91–102

Bashan A, Yonath A (2008) Correlating ribosome function with high-resolution structures. Trends Microbiol 16(7):326–335

Beckmann R, Bubeck D, Grassucci RA, et al (1997) Alignment of conduits for the nascent polypeptide chain in the ribosome-Sec61 complex. Science 278 (5346)

Belardinelli R, Sharma H, Caliskan N et al (2016) Choreography of molecular movements during ribosome progression along mRNA. Nat Struct Mol Biol 23:342–348

Bernabeu C, Lake JA (1982) Nascent polypeptide chains emerge from the exit domain of the large ribosomal subunit: immune mapping of the nascent chain. Proc Natl Acad Sci USA 79:3111–3115

Bhushan S, Hoffmann T, Seidelt B et al (2011) SecM-stalled ribosomes adopt an altered geometry at the peptidyl transferase center. PLoS Biol 9 (1)

Brosius J, Palmer ML, Kennedy PJ et al (1978) Complete nucleotide sequence of 16S ribosomal RNA gene from *Escherichia coli*. Proc Nat Acad Sci USA 75:4801–4805

Buhr F, Jha S, Thommen M et al (2016) Synonymous codons direct cotranslational folding toward different protein conformations. Mol Cell 61:341–351

Cabrita LD, Cassaignau AM, Launay HM et al (2016) A structural ensemble of a ribosome-nascent chain complex during cotranslational protein folding. Nat Struct Mol Biol 23(4):278–285

Carter AP, Clemens WM, Brodersen DE et al (2000) Functional insights from the structure of the 30S ribosomal subunit and its interactions with antibiotics. Nature 407(6802):340–348

Chen B, Kaledhonkar S, Sun M et al (2015) Structural dynamics of ribosome subunit association studied by mixing-spraying time-resolved cryogenic electron microscopy. Structure 23 (6):1097–1105

Christodoulou J, Larsson G, Fucini P et al (2004) Heteronuclear NMR investigations of dynamic regions of intact *Escherichia coli* ribosomes. Proc Natl Acad Sci USA 101(30):10949–10954

Clarke TF, Clark PL (2008) Rare codons cluster. PLoS ONE 3:e3412

Clore GM, Gronenborn AM (1998) New methods of structure refinement for macromolecular structure determination by NMR. Proc Natl Acad Sci USA 95(11):5891–5898

Cornish PV, Ermolenko DN, Noller HF et al (2008) Spontaneous intersubunit rotation in single ribosomes. Mol Cell 30(5):578–588

Deckert A, Waudby CA, Wlodarski T et al (2016) Structural characterization of the interaction of α-synuclein nascent chains with the ribosomal surface and trigger factor. Proc Natl Acad Sci USA 113(18):5012–5017

Delius H, Traut RR, Moore PB et al (1968) Studies on purified *E.coli* ribosomal proteins. Molecular Genetics, Springer-Verlag, Berlin, pp 26–45

Demo G, Rasouly A, Vasilyev N et al (2017a) Structure of RNA polymerase bound to ribosomal 30S subunit. Elife. 6:e28560

Demo G, Svidritskiy E, Madireddy R et al (2017b) Mechanism of ribosome rescue by ArfA and RF2. Elife. 6

Diaconu M, Kothe U, Schluenzen F et al (2005) Structural basis for the function of the ribosomal L7/L12 stalk in factor binding and GTPase activation. Cell 121(7):991–1004

Doerfel LK, Wohlgemuth I, Kubyshkin V et al (2015) Entropic contribution of elongation factor P to proline positioning at the catalytic center of the ribosome. J Am Chem Soc 137:12997–13006

Dubochet J, Adrian M, Chang JJ et al (1988) Cryo-electron microscopy of vitrified specimens. Q Rev Biophys 21(2):129–228

Dunkle JA, Wang L, Feldman MB et al (2011) Structures of the bacterial ribosome in classical and hybrid states of tRNA binding. Science 332(6032):981–984

Elad N, Clare D, Saibil HR et al (2008) Detection and separation of heterogeneity in molecular complexes by statistical analysis of their two-dimensional projections. J Struct Biol 162:108–120

Eyal Z, Matzov D, Krupkin M et al (2015) Structural insights into species-specific features of the ribosome from the pathogen Staphylococcus aureus. Proc Natl Acad Sci 112(43):5805–5814

Fischer N, Konevega AL, Wintermeyer W et al (2010) Ribosome dynamics and tRNA movement by time-resolved electron microscopy. Nature 466(7304):329–33

Frank J, Penczek P, Grassucci RA et al (1991) Three-dimensional reconstruction of the 70S *Escherichia coli* ribosome in ice: the distribution of ribosomal RNA. J Cell Biol 115(3):597–605

Frank J (2017) Time-resolved cryo-electron microscopy: recent progress. J Struct Biol 3:303–306

Frank J (2006) Three-dimensional electron microscopy of macromolecular assemblies: visualization of biological molecules in their native state. Oxford University Press: Chapter 2:20–40

Frank J, Agrawal RK (1998) The movement of tRNA through the ribosome. Biophys J 74(1):589–594

Frank J, Agrawal RK (2000) A ratchet-like inter-subunit reorganization of the ribosome during translocation. Nature 406(6793):318–322

Frank J, Zhu J, Penczek P et al (1995) A model of protein synthesis based on cryo-electron microscopy of the *E. coli* ribosome. Nature 376(6539):441–444

Fu Z, Kaledhonkar S, Borg A et al (2016) Key intermediates in ribosome recycling visualized by time-resolved cryoelectron microscopy. Structure 24(12):2092–2101

Gabashvili IS, Agrawal RK, Spahn CM et al (2000) Solution structure of the *E. coli* 70S ribosome at 11.5 A resolution. Cell 100(5):537–549
Gabashvili IS, Gregory ST, Valle M et al (2001) The polypeptide tunnel system in the ribosome and its gating in erythromycin resistance mutants of L4 and L22. Mol Cell 8(1):181–188
Gao H, Zhou Z, Rawat U et al (2007) RF3 induces ribosomal conformational changes responsible for dissociation of class I release factors. Cell 129(5):929–941
Gao N, Zavialov AV, Li W et al (2005) Mechanism for the disassembly for the posttermination complex inferred from cryo-EM studies. Mol Cell 18(6):663–674
Goyal A, Belardinelli R, Rodnina MV (2017) Non-canonical binding site for bacterial initiation factor 3 on the large ribosomal subunit. Cell Rep. 20(13):3113–3122
Graf M, Huter P, Maracci C et al (2018) Visualization of translation termination intermediates trapped by the Apidaecin 137 peptide during RF3-mediated recycling RF1. Nat Comm. 9 (1):3053
Green R, Noller HF (1997) Ribosomes and translation. Annu Rev Biochem 66:679–716
Guo Z, Noller HF (2012) Rotation of the head of the 30S ribosomal subunit during mRNA translocation. Proc Natl Acad Sci 109:20391–20394
Hope H, Frolow F, Bohlen K et al (1989) Cryocrystallography of ribosomal particles. Acta Crystallogr Sect B 45:190–199
Harms J, Schluenzen F, Zarivach R et al (2001) High resolution structure of the large ribosomal subunit from a mesophilic eubacterium. Cell 107(5):679–688
Henderson R (2015) Overview and future of single particle electron cryomicroscopy. Arch Biochem Biophys 581:19–24
Hentschel J, Burnside C, Mignot I et al (2017) The complete structure of the *Mycobacterium smegmatis* 70S Ribosome. Cell. Rep. 20(1):149–160
Herr W, Noller HF (1975) A fragment of 23S RNA containing a nucleotide sequence complementary to a region of 5S RNA. FEBS Lett 53:248–252
Huter P, Arenz S, Bock LV et al (2017a) Structural basis for polyproline-mediated ribosome stalling and rescue by the translation elongation factor EF-P. Mol Cell 68:515–527.e516
Huter P, Muller C, Beckert B et al (2017b) Structural basis for ArfA-RF2-mediated translation termination on mRNAs lacking stop codons. Nature 541(7638):546–549
Ingolia NT, Hussmann JA, Weissman JS (2019) Ribosome Profiling: Global views of Translation. Cold Spring Harb Perspect Biol 11(5) pii:a032698
James NR, Brown A, Gordiyenko Y et al (2016) Translational termination without a stop codon. Science 354(6318):1437–1440
Javed A, Christodoulou J, Cabrita et al (2017) The ribosome and its role in protein folding: looking through a magnifying glass. Acta Cryst D Struc Biol 73(Pt6):509–521
Javed A, Cabrita D. Lisa, Cassaignau ME A, Wlodarski T, Christodoulou J, Orlova EV (2019) Visualising nascent chain dynamics at the ribosome exit tunnel by cryo-electron microscopy. BioRxiv. https://doi.org/10.1101/722611
Jin H, Kelley AC, Ramakrishnan V (2011) Crystal structure of the hybrid state of ribosome in complex with the guanosine triphosphatase release factor 3. Proc Natl Acad Sci 108 (38):15798–15803
Julian P, Milon P, Agirrezabala X et al (2011) The Cryo-EM structure of a complete 30S translation initiation complex from Escherichia coli. PLoS Biol 9(7):e1001095
Kaminishi T, Wilson DN, Takemoto C et al (2007) A snapshot of the 30S ribosomal subunit capturing mRNA via the Shine-Dalgarno interaction. Structure 15(3):289–297
Khusainov I, Vicens Q, Bochler A et al (2016) Structure of the 70S ribosome from human pathogen *Staphylococcus aureus*. Nuc Acid Res. 44(21):10491–10504
Kohler R, Mooney RA, Mills DJ et al (2018) Architecture of a transcribing-translating expressome. Science 356(6334):194–197
Korostelev A, Asahara H, Lancaster L et al (2008) Crystal structure of a translation termination complex formed with release factor RF2. Proc Natl Acad Sci 105(50):19684–19690
Korostelev A, Trakhanov S, Laurberg M et al (2006) Crystal structure of a 70S ribosome-tRNA complex reveals functional interactions and rearrangements. Cell 126(6):1065–1077

Korostelev A, Zhu J, Asahara H et al (2010) Recognition of the amber UAG stop codon by release factor RF1. EMBO J 29:2577–2585
Kothe U, Widen HJ, Mohr D et al (2004) Interaction of helix D of elongation factor Tu with helices 4 and 5 of protein L7/L12 on the ribosome. J Mol Biol 336(5):1011–21
Lake JA (1978) Protein synthesis. Science 200(4339):305–306
Laurberg M, Asahara H, Korostelev A et al (2008) Structural basis for translation termination on the 70S ribosome. Nature 454:852–857
Li W. McClure K, Montabana E et al (2018) Structural basis for selective stalling of human ribosome nascent chain complexes by a drug-like molecule. bioRxiv. https://doi.org/10.1101/315325
Ling C, Ermolenko DN (2016) Structural insights into ribosome translocation. Wiley Interdiscip Rev RNA. 5:620–36
Liu Q, Frederick K (2016) Intersubunit Bridges of the Bacterial Ribosome. J Mol Biol 428(10 Pt B): 2146–2164
Lopez-Alonso JP, Fabbretti A, Kaminishi T et al (2017) Structure of a 30S pre-initiation complex stalled by GE81112 reveals structural parallels in bacterial and eukaryotic protein synthesis initiation pathways. Nucleic Acids Res 45(4):2179–2187
Loveland AB, Demo G, Grigorieff N et al (2017) Ensemble cryo-EM elucidates the mechanism of translation fidelity. Nature 546:113–117
Marzi S, Knight W, Brandi L, Caserta E, Soboleva N, Hill WE, Gualerzi CO, Lodmell JS (2003) Ribosomal localization of translation initiation factor IF2. RNA 9(8):958–969
Marzi S, Myasnikov AG, Serganov A et al (2007) Structured mRNAs regulate translation initiation by binding to the platform of the ribosome. Cell 130(6):1019–1031
Matadeen R, Patwardhan A, Gowen B et al (1999) The *Escherichia coli* large ribosomal subunit at 7.5 A resolution. Structure 7 (12):1575–83
McCutcheon JP, Agrawal RK, Philips SM et al (1999) Location of translational initiation factor IF3 on the small ribosomal subunit. Proc Natl Acad Sci 96:4301–4306
Melnikov S, Ben-Shem A, Gareau de Loubresse N et al (2012) One core, two shells: bacterial and eukaryotic ribosomes. Nat Struct Mol Biol 19(6):560–567
Melnikov S, Manakongtreecheep K, Soll D (2018) Revising the structural diversity of ribosomal proteins across the three domains of life. Mol Biol and Evol. 35(7):1588–1598
Midgley JEM (1965) Effects of different extraction procedures on the molecular characteristics of bacterial ribosome ribonucleic acid. Biochem Biophys Acta 95:232–243
Milligan RA, Unwin PN (1986) Location of exit channel for nascent protein in 80S ribosome. Nature 319:693–695
Moller K, Brimacombe R (1975) Specific cross-linking of proteins S7 and L4 to ribosomal RNA, by UV irradiation of *Escherichia coli* ribosomal subunits. Mol Gen Genet 141(4):343–345
Moore PB (2009) The ribosome returned. J Biol. 8(1):1–8
Moore PB, Engelman DM (1975) A neutron scattering study of the distribution of protein and RNA in the 30S ribosomal subunit of *Escherichia coli*. J Mol Biol 91:101–120
Moore PB, Traut RR, Noller HF et al (1968) Ribosomal proteins of *Escherichia coli*. II. Proteins from the 30S subunit. J Mol Biol 31:441–461
Myasnikov AG, Marzi S, Simonetti A et al (2005) Conformational transition of initiation factor 2 from the GTP—to-GDP-bound state visualised on the ribosome. Nat Struct Mol Biol 12 (12):1145–1149
Nilsson OB, Nickson AA, Hollins JJ et al (2017) Cotranslational folding of spectrin domains via partially structured states. Nat Struct Mol Biol 24(3):221–225. https://doi.org/10.1038/nsmb.3355
Nilsson OB, Hedman R, Marino J et al (2015) Cotranslational protein folding inside the ribosome exit tunnel. Cell Rep. 12(10):1533–1540
Nissen P, Hansen J, Ban N et al (2000) The structural basis of ribosome activity in peptide bond synthesis. Science 289(5481):920–930
Noller, H.F. and Herr, W. (1974). Accessibility of 5S rRNA in 50S ribosomal subunits. J Mol Biol 90:181–184

Noeske J, Wasserman MR, Terry DS et al (2015) High-resolution structure of the *Escherichia coli* ribosome. Nat Struct Mol Biol 22(4):336–341
O'Brien EP, Ciryam P, Vendruscolo M et al (2014) Understanding the influence of codon translation rates on cotranslational protein folding. Acc Chem Res 47:1536–1544
Ogle JM, Murphy FV, Tarry MJ et al (2002) Selection of tRNA by the ribosome requires a transition from an open to a closed form. Cell 111:721–732
Ogle JM, Ramakrishnan V (2005) Structural insights into translational fidelity. Annu Rev Biochem 74:129–177
Orlova EV (2000) Structural analysis of non-crystalline macromolecules: the ribosome. Acta Crystallogr D Biol Crystallogr 56:1253–8
Palade GE (1955) A small particulate component of the cytoplasm. J Biophys Biochem Cytol 1:59–68
Pallesen J, Hashem Y, Korkmaz G et al (2013) Cryo-EM visualization of ribosome in termination complex with apo-RF3 and RF1. Elife 2
Peske F, Rodnina MV, Wintermeyer W (2005) Sequence of steps in ribosome recycling as defined by kinetic analysis. Mol Cell 18(4):403–412
Petrov A, Chen J, O'Leary S et al (2012) Single-molecule analysis of translational dynamics. Cold Spring Harb Perspective Biol. 4(9):a011551. https://doi.org/10.1101/cshperspect.a011551
Polacek N, Mankin AS (2005) The ribosomal peptidyl transferase center: structure, function, evolution, inhibition. Crit Rev Biochem Mol Biol 40(5):285–311
Polacek N, Gaynor M, Yassin A et al (2001) Ribosomal peptidyl transferase can withstand mutations at the putative catalytic nucleotide. Nature 411:498–501
Polikanov YS, Steitz TA, Innis CA (2014) A proton wire to couple aminoacyl-tRNA accommodation and peptide-bond formation on the ribosome. Nat Struct Mol Biol 21 (9):787–93
Rawat U, Gao H, Zavialov A et al (2006) Interactions of the release factor RF1 with the ribosome as revealed by cryo-EM. J Mol Biol 357:1144–1153
Rawat UBS, Zavialov AV, Sengupta J et al (2003) A cryo-electron microscopic study of ribosome-bound termination factor RF2. Nature 421:87–90
Rodnina MV (2018) Translation in Prokaryotes. Cold Spring Harb Perspect Biol 10(9):1–21
Santos N, Zhu J, Donohue PJ et al (2013) Crystal structure of the 70S ribosome bound with Q253P mutant form of release factor RF2. Structure 21(7):1258–1263
Savelsbergh A, Katunin VI, Mohr D et al (2003) An elongation factor G-induced ribosome rearrangement precedes tRNA-mRNA translocation. Mol Cell 11:1517–1523
Schmeing TM, Ramakrishnan V (2009) What recent ribosome structures have revealed about the mechanism of translation. Nature 461(7268):1234–42
Schmeing TM, Voorhees RM, Kelley AC et al (2009) The crystal structure of the ribosome bound to EF-Tu and aminoacyl-tRNA. Science 326(5953):688–694
Seidelt B, Innis CA, Wilson DN et al (2009) Structural insight into nascent polypeptide chain-mediated translational stalling. Science 326(5958):1412–1415
Selmer M, Dunham CM, Murphy FV 4th et al (2006) Structure of the 70S ribosome complexed with mRNA and tRNA. Science 313(5795):1935–1942
Shaikh TR, Yassin AS, Lu Z et al (2014) Initial bridges between two ribosomal subunits are formed within 9.4 milliseconds, as studied by time-resolved cryo-EM. Proc Natl Acad Sci. 111 (27):9822–9827
Siller E, DeZwaan DC, Anderson JF et al (2010) Slowing bacterial translation speed enhances eukaryotic protein folding efficiency. J Mol Biol 396:1310–1318
Simonetti A, Marzi S, Myasnikov AG et al (2008) Structure of the 30S initiation complex. Nature 455(7211):416–420
Sohmen D, Chiba S, Shimokawa-Chiba N et al (2015) Structure of the Bacillus subtilis 70S ribosome reveals the basis for species-specific stalling. Nat Commun 6:6941. https://doi.org/10.1038/ncomms7941
Spencer PS, Siller E, Anderson JF et al (2012) Silent substitutions predictably alter translation elongation rates and protein folding efficiencies. J Mol Biol 422:328–335

Sprink T, Ramrath D, Yamamoto H et al (2016) Structures of ribosome-bound initiation factor 2 reveal the mechanism of subunit association. Sci Adv. 2(3):e1501502

Stark H, Orlova EV, Rinke-Appel J et al (1997) Arrangement of tRNAs in pre- and posttranslational ribosomes revealed by electron cryomicroscopy. Cell 88:19–28

Stark H, Rodnina MV, Wieden HJ et al (2002) Ribosome interactions of aminoacyl-tRNA and elongation factor Tu in the codon-recognition complex. Nat Struct Biol 9:849–854

Steitz TA (2008) A structural understanding of the dynamic ribosome machine. Nat Rev Mol Cell Biol 9(3):242–253

Svidritskiy E, Korostelev A (2018) Conformational control of translation termination on the 70S ribosome. Structure. 26(6):821–828

Taylor MM, Glasgow JE, Storck R (1967) Sedimentation coefficients of RNA from 70S and 80S ribosomes. Proc Natl Acad Sci U S A. 57(1):164–9

Tian P, Steward A, Kudva R et al (2018) Folding pathway of an Ig domain is conserved on and off the ribosome. Proc Natl Acad Sci 115(48):E11284–E11293

Tischendorf GW, Zeichhardt H, Stoffler G (1974a) Determination of the location of proteins L14, L17, L18, L19, L22, L23 on the surface of 50S ribosomal subunit of *Escherichia coli* by immune electron microscopy. Mol Gen Genet 134:187–208

Tischendorf GW, Zeichhardt H, Stoffler G (1974b) Location of proteins, S5, S13 and S14 on the surface of the 30S ribosomal subunit from *Escherichia coli* as determined by immune electron microscopy. Mol Gen Genet 134:209–223

Tissieres A, Watson JD (1958) Ribonucleoprotein particles from the *Escherichia coli*. Nature 182 (4638):778–780

Tsai CJ, Sauna ZE, Kimchi-Sarfaty C et al (2008) Synonymous mutations and ribosome stalling can lead to altered folding pathways and distinct minima. J Mol Biol 383:281–291

Valle M, Zavialov A, Li W et al (2003) Incorporation of aminoacyl-tRNA into the ribosome as seen by cryo-electron microscopy. Nat Struct Biol 10:899–906

Vesper O, Amitai S, Belitsky M et al (2011) Selective translation of leaderless mRNAs by specialised ribosomes generated by MazF in *Escherichia coli*. Cell 147(1):147–157

Wasserman MR, Alejo JL, Altman RB et al (2016) Multiperspective smFRET reveals rate-determining late intermediates of ribosomal translocation. Nat Struct Mol Biol 23:333–341

Weixlbaumer A, Jin H, Neubauer C et al (2008) Insights into translational termination from the structure of RF2 bound to the ribosome. Science 322:953–956

Wilson DN, Arenz S, Beckmann R (2016) Translation regulation via nascent polypeptide-mediated ribosome stalling. Curr Opin Struct Biol 37:123–33

Wimberly BT, Brodersen DE, Clemons WM Jr (2000) Structure of the 30S ribosomal subunit. Nature 407(6802):327–339

Yonath A, Leonard RK, Wittmann GH (1987) A tunnel in the large ribosomal subunit revealed by three-dimensional image reconstruction. Science 236:813–6

Yu CH, Dang Y, Zhou Z et al (2015) Codon usage influences the local rate of translation elongation to regulate co-translational protein folding. Mol Cell 59:744–754

Yusupov M, Yusupova G, Baucom A et al (2001) Crystal structure of the ribosome at 5.5 A resolution. Science. 292(5518):883–96

Zavialov AV, Hauryliuk VV, Ehrenberg M (2005) Splitting of the posttermination ribosome into subunits by the concerted action of RRF and EF-G. Mol Cell 18(6):675–686

Zhang G, Hubalewska M, Ignatova Z (2009) Transient ribosomal attenuation coordinates protein synthesis and co-translational folding. Nat Struc Mol Biol. 16(3):274–80

Zhou J, Lancaster L, Donohue JP et al (2019) Spontaneous ribosomal translocation of mRNA and tRNAs into a chimeric hybrid state. Proc Natl Acad Sci.. https://doi.org/10.1073/pnas.1901310116